Article

Homogeneous entropy catalytic-driven DNA hydrogel as strong signal blocker for highly sensitive electrochemical detection of platelet-derived growth factor

Yuanyuan Chang, Mengyao Li, Zhongyu Wu, Ying Zhuo, Yaqin Chai, Qi Xiao, and Ruo Yuan

Anal. Chem., **Just Accepted Manuscript** • DOI: 10.1021/acs.analchem.8b01766 • Publication Date (Web): 07 Jun 2018

Homogeneous entropy catalytic-driven DNA hydrogel as strong signal blocker for highly sensitive electrochemical detection of platelet-derived growth factor

Yuanyuan Chang,[†] Mengyao Li,[†] Zhongyu Wu,[†] Ying Zhuo,[†] Yaqin Chai,[†] Qi Xiao,*[‡] Ruo Yuan*[†]

[†] *Key Laboratory of Luminescent and Real-Time Analytical Chemistry (Southwest University), Ministry of Education, College of Chemistry and Chemical Engineering, Southwest University, Chongqing 400715, PR China*

[‡] *College of Chemistry and Materials Science, Guangxi Teachers Education University, Nanning 530001, PR China*

[*]Corresponding authors at: Tel.: +86-23-68252277, fax: +86-23-68253172.
E-mail addresses: qi.xiao@whu.edu.cn (Q. Xiao); yuanruo@swu.edu.cn (R. Yuan).

ABSTRACT

In this work, an elegantly designed electrochemical biosensor was constructed for platelet-derived growth factor (PDGF) detection based on homogeneous entropy catalytic-induced DNA hydrogel as strong signal blocker to significantly inhibit the electrochemical signal of g-C_3N_4@Au@Fc-NH_2 nanomaterials as signal tag. First, the well film-forming nanomaterials of g-C_3N_4@Au@Fc-NH_2 containing large numbers of Fc-NH_2 with low resistance and high electric conductivity were directly immobilized on electrode surface to provide strong original electrochemical signal, then DNA hydrogel blocker formed by target-induced homogeneous entropy catalytic amplification was captured onto the modified electrode surface for significantly reducing the electrochemical signal, in which both the efficient conversion of the single protein to large numbers of DNA strands and the amplification of cycling products could doubly improve the detection sensitivity. As a result, the detection limit could reach to 3.5 fM at the range of 0.01 pM to 10 nM. The present strategy by integration of strong signal blocker to sharply reduce the electrochemical signal of signal tag initiates a new thought to realize the highly sensitive detection of biomarkers and possesses the potential applications in clinical diagnosis, sensing and other related subjects.

KEYWORDS: nanomaterials, carbon nitride, aminoferrocenec acid, homogeneous entropy catalytic, DNA hydrogel

Strategies to immobilize molecules or nanomaterials with well electroactivities onto electrode surface is significant for characterizing the changes after different substances was introduced in biosensor for target detection.[1,2] There have been developed several immobilization methods to tailor surfaces for a variety of diagnostic and high-throughput assays,[3-5] including direct and indirect immobilization. Nafion and chitosan are usually used as well film-forming substance for direct immobilizing signal tag, for example, hemin,[6] $K_3[Fe(CN)_6]$,[7] ferrocene (Fc),[8] etc, but the low-efficiency signal output of signal tag lead to the weak original electrochemical signal owing that electrically inert molecules of nafion and chitosan could seriously hinder the electron transfer, resulting the decreased detection accuracy. Moreover, the electro-deposition approach is also adopted to directly immobilize signal tag for the construction of electrochemical biosensor, however, this method needs special condition and may result in low sensitivity and stability of the biosensor, for example, prussian blue by electro-deposition could easily diffuse away from the electrode surface into the bulk solution,[9,10] leading to low stability and signal output intensity. While, labeling, embedding and adsorbing are the most popular methods to indirectly immobilize signal tags onto the electrode surface, such as, methylene blue (MB), Fc, etc.[11-13]Although these methods could overcome the difficulty immobilization of some signal tags and provide guiding way to capture other potential signal tags, the complex label, inevitable background signal and weak original signal limit their further applications. Based on the above analysis, to avoid

these disadvantages, it is imperative to develop the electrode materials with high-throughput, high-performance and well film-forming nanomaterials but at a low cost to be directly immobilized on the electrode surface as signal tag to short electron and ion transport pathways and provide strong initial output signal for improving the detention accuracy and the utility of electrode surfaces.

In traditional biosensors for protein detection, the target is commonly recognized by a fixed recognition element immobilized on a solid support, thus the number of available recognition elements is limited, leading that the quantity of target protein recognized reduces correspondingly, finally the detection sensitivity decreases.[14,15] Moreover, these methods for the immobilization of protein encounter with another problem involving the increase of generated nonspecific signal without complex separation and washing steps, resulting in the speed for target detection being restricted.[16-18] Therefore, seeking out appropriate path to overcome the above difficulties is still an inevitable challenge in protein detection. Recently, a lot of efforts are devoted to improving the present situation,[19,20] for example, the proximity ligation assay (PLA) in homogeneous solution which was developed to transduce targets input into nucleic acid output has obtained more attentions due to the fact that it could reach the similar level of performance without utilizing a solid support, and improve detection speed and automation.[21-23] Kim groups have designed a homogeneous entropy catalytic-driven amplified detection for sensing purpose, overcoming the difficulties of only capable of nucleic acid recycling, the generated signal without amplification and time-consuming in most homogeneous assays.[24]

Although the results were satisfied, the wide application of this method were still suppressed by complex label and the detection object of only cycling products without any amplifications, leading to the limited detection sensitivity. Because of these, the demand for applying homogeneous assay to detect protein with simple, high effective and sensitivity has urgently risen.

DNA hydrogels, which consist of large numbers of DNA strands, could be used as excellent blocker to hinder electron transfer, thus they have been applied in electrochemical biosensors for sensitive detection of target.[25,26] Commonly, DNA hydrogels were manipulated by physical entanglement, chemical crosslinking, electrostatic interaction or enzymatic ligation to form two- or three-dimensional geometric nanostructures or periodic arrays.[27,28] Unfortunately, these methods are confined by the active of ligase, strict specific conditions, requirement of a large amount of DNA, environmentsensitive disassembly and low efficiency. While adopting DNA hybridization based on Watson-Crick base-pairing to form DNA hydrogels has been applied in wide range in recent years due to its easy operation, high efficiency and universal condition.[29,30] Nucleic acid hairpin structure is usually as the best candidate to yield DNA hydrogels owing that it could perform as catalytic energetic traps which are able to be activated via an initiator with the help of a free-energy driven isothermal autonomous catalytic hairpin assembly process.[31,32] However, the DNA hydrogels formed with these reactions are usually under non-homogeneous condition, which led to unnecessary assembly, laborious purification steps and high cost. Therefore, how to overcome these disadvantages for

improving the efficiency to form DNA hydrogels with good performance is still an urgent need.

Herein, homogeneous entropy catalytic-triggered strategy was designed for the formation of DNA hydrogel to amplify the cycling products for powerful restrain the strong initial signal of well film-forming functionalized nanomaterials g-C_3N_4@Au@Fc-NH_2 in an electrochemical biosensor for sensitive detection of PDGF. The detection principle was displayed in Scheme 1. Firstly, two well-designed DNA structures including template and A1 were mixed for forming A1-template, while synchronous binding of the catalytic probe pairs (S1 and S2) to one target protein molecule (S1-target-S2) triggered the displacement of the blocker A1 sequence from the A1-template and the exposure of the prelocked toehold region for the formation of Intermediate Substrate (IS) structure. Subsequent fuel DNA compelled S1-target-S2 and another A1 sequence to be released, at this time, S1-target-S2 could be used as recycling structure for amplifying electrochemical signal, and the released two A1 sequences could open two hairpin DNA (HP1 and HP2) for the formation of DNA hydrogels with the help of phi-29 and dNTPs. The formed DNA hydrogels were captured onto the electrode surface by complementary base pairing with A2 and A3, leading to the significant decrease in electrochemical signal and realizing the sensitive detection of protein. In short, the proposed biosensor combining homogeneous entropy catalytic-induced DNA hydrogel to strongly hinder the electrochemical signal of g-C_3N_4@Au@Fc-NH_2 nanomaterials offers a new way to sensitively detect PDGF or other biomarkers.

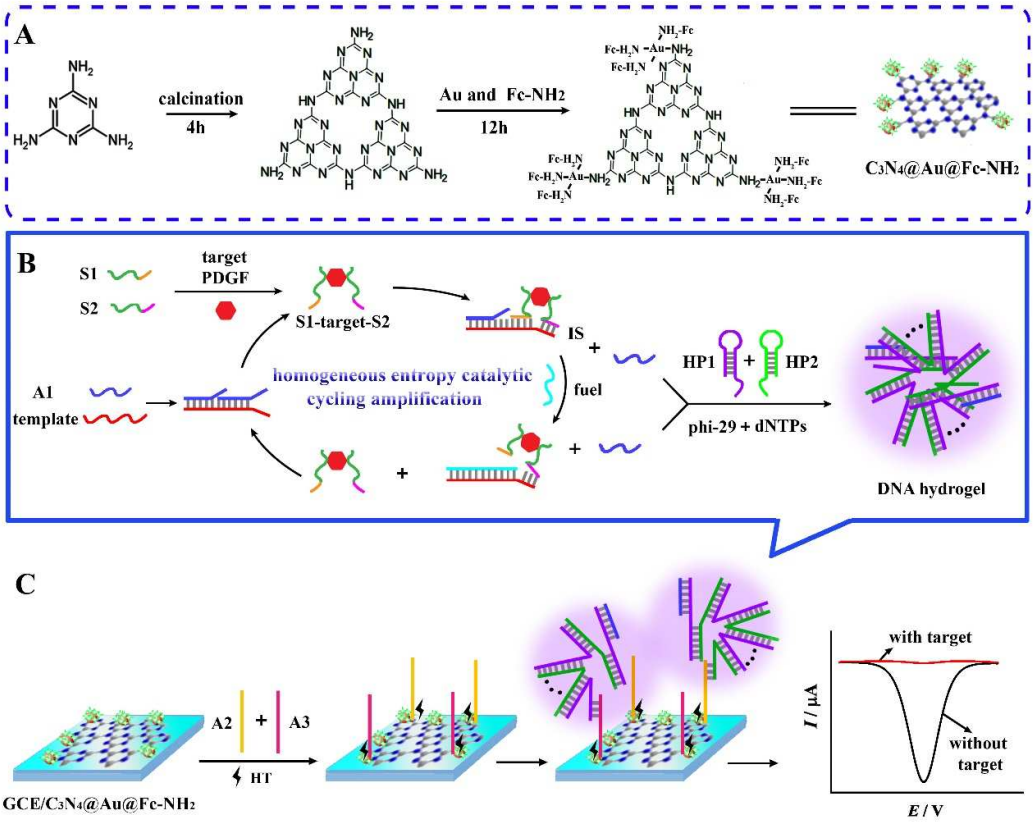

Scheme 1 (A) The preparation of electroactive g-C_3N_4@Au@Fc-NH_2 nanomaterials, (B) the formation of DNA hydrogel based on homogeneous entropy catalytic amplification, (C) the construction of the proposed biosensor for PDGF detection based on homogeneous entropy catalytic-driven DNA hydrogel as strong signal blocker to significantly inhibit the electrochemical signal of electroactive g-C_3N_4@Au@Fc-NH_2 nanomaterials.

EXPERIMENTAL SECTION

Preparation of g-C_3N_4 and g-C_3N_4@Au@Fc-NH_2 Nanomaterials g-C_3N_4 was synthesized by the previous method of calcining melamine with some modifications.[33] First, melamine (6.0 g) was put in a semi-closed alumina crucible and heated to 520 °C for 4 h with the heating rate at 10 °C/min. Then, cooled down to room

temperature, and bright yellow powder of g-C_3N_4 was obtained. The prepared 10 mg g-C_3N_4 yellow powder was dispersed into 2 mL ultrapure water and added 10 mg aminoferrocenec acid (Fc-NH_2), then sonicated until uniformly dispersed. Next, 500 μL nano-Au was introduced into this as-prepared solution and mixed under magnetic stirring for 14 h. Finally, the solution was centrifuged and washed with doubly distilled water for several times for obtaining g-C_3N_4@Au@Fc-NH_2 nanomaterials owing that the NH_2 of g-C_3N_4 and Fc-NH_2 could combine with nano-Au for the formation of Au-N bonding.

Homogeneous Entropy Catalytic Cycling Amplification Before using, the hairpin DNA sequences including A2, A3, HP1 and HP2 were dealt with annealing. Firstly, A1 (5.0 μM) was mixed with template (2.5 μM) for 2 h, and target (10 pM) mixed with S1 (2.5 μM) and S2 (2.5 μM) for 100 min respectively. Then, the above two mixtures reacted together for 80 min. Subsequently, fuel DNA sequence was added for 2 h to form template-fuel dsDNA. Afterward, two annealed hairpin DNA sequences including HP1 and HP2 were mixed with the obtained mixture for 2 h under phi-29 polymerase (1 U/uL) and dNTPs (1 mM).

The Fabrication of the Modified Electrodes Firstly, 10 μL electroactive nanomaterials of g-C_3N_4@Au@Fc-NH_2 was dropped on the electrode surface and dried in the room temperature, then introduced A2 and A3 into this system via Au-N bond for 16 h. Next, 15 μL HT was immobilized on the modified electrode surface for 50 min. Finally, the products obtained from homogeneous entropy catalytic amplification were adopted on the modified electrode surface for 2 h. All steps were

washed with ultrapure water respectively, and the prepared electrode was used for electrochemical measurements.

RESULTS AND DISCUSSIONS

Characterization of g-C_3N_4 and g-C_3N_4@Au@Fc-NH_2 Nanomaterials To prove that the nanomaterials used in this work were successfully synthesized, scanning electron microscope (SEM) was performed and the results were displayed in Figure 1. As can be seen, the nano-Au with uniform spherical morphology was appeared in the Figure 1A, and the inset was the TEM morphology which was according to the SEM morphology of nano-Au. The g-C_3N_4 displayed typical two-dimensional (2D) lamellar structures in Figure 1B. Once the nano-Au and Fc-NH_2 were introduced, an amount of nanoparticles were aggregated in edge of g-C_3N_4 (Figure 1C), which proved to the successful binding between g-C_3N_4 and nano-Au. While the nano-Au turned from spherical to nanoflower morphology, demonstrating that the Fc-NH_2 was also successfully immobilized on the surface of nano-Au. From these results, we could conclude that the g-C_3N_4@Au@Fc-NH_2 nanomaterials were successfully synthesized.

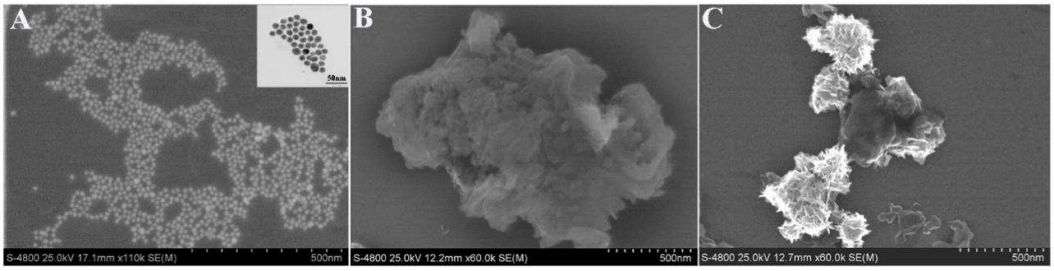

Figure 1. (A) The SEM characterization of nano-Au (A), g-C_3N_4 (B) and g-C_3N_4@Au@Fc-NH_2 nanomaterials (C). The inset was the TEM characterization of nano-Au.

The Optimization of the Experimental Conditions Since the driving force for homogeneous entropy catalytic amplification was depended on the reaction of S1,

target and S2, thus, we optimized the incubation time for the formation of S1-target-S2. As the Figure 2A displayed, with incubation time increasing, the electrochemical signal increased and then reached a platform at 100 min. Therefore, in order to obtain best results for homogeneous entropy catalytic amplification, 100 min was chosen as the optimal incubation time for S1, target and S2. Moreover, the reaction between S1-target-S2 and A1-template was an important procedure for releasing A1 to participate in the formation of DNA hydrogel, thus the optimizing incubation time of S1-target-S2 and A1-template was performed. Figure 2B illustrated that the signal current raised as time went on until 80 min, as a consequence, 80 min was conducted as the optimal incubation time for S1-target-S2 and A1-template. In addition, the formation of DNA hydrogel played a significant role in the whole

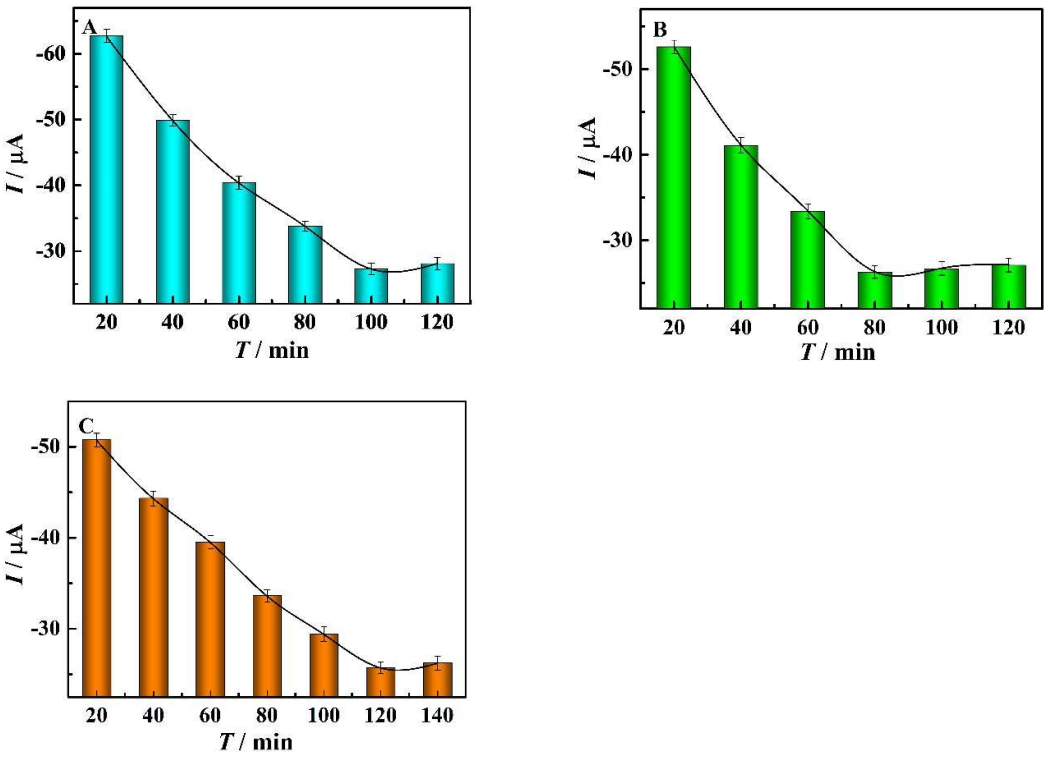

Figure 2 (A) Optimum reaction time for the formation of (A) S1-target-S2, (B) IS structure, (C)

DNA hydrogel.

experiment which could effect the sensitivity and linearity range for the target detection. Consequently, the optimization of time for HP-A and HP-B in presence of phi-29 and dNTPs to generate DNA hydrogel was operated. From the Figure 2C, we could see that the electrochemical signal for g-C_3N_4@Au@Fc-NH_2 augmented with the incubation time gradually, until the incubation time reached at 120 min, good gradient for the current signal was obtained. Thus 120 min was adopted as the most appropriate incubation time to form DNA hydrogel.

Electrochemical Characterization of the Proposed Biosensor The fabrication of this proposed biosensor for PDGF detection was recorded with SWV measurement in 2 mL PBS solution (pH 7.0). As is displayed in Figure 3A, when the bare GCE was detected, no electrochemical signal appeared due to the lack of electroactivities (curve a). Once the g-C_3N_4@Au@Fc-NH_2 nanomaterials was introduced onto electrode surface, an obvious oxidative peak was obtained (curve b), demonstrating that g-C_3N_4@Au@Fc-NH_2 possesses good film-forming and electroactivities which could act as signal tag. Because DNA strand could hinder the electron transfer, when A2 and A3 were immobilized on the modified electrode surface via Au-N bond, the current signal reduced (curve c). When HT was introduced to block the non-special bonding sites, the signal further decreased as we aspect (curve d). While the formed DNA hydrogel was adopted onto the as-prepared electrode, the current peak was noticeably decreased (curve e), attributing that the formed DNA hydrogel was consist of large numbers of DNA strands and able to impede the electron transfer intensively.

Moreover, the cyclic voltammetry (CV) experiment was carried out for further demonstrating the successful construction of this strategy and the related contents were seen in Supporting Information.

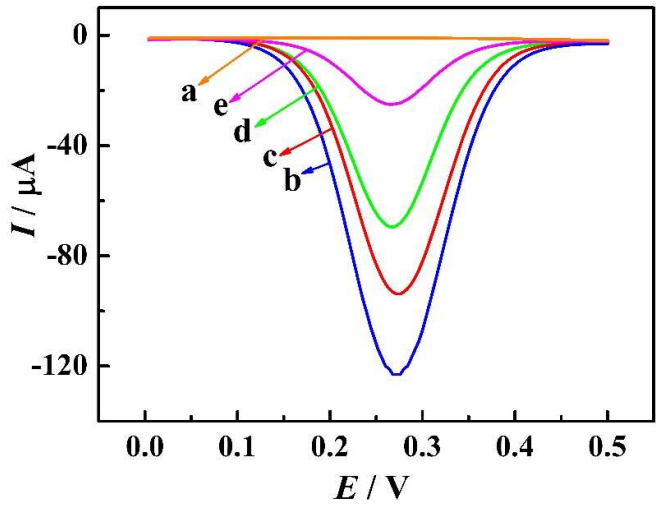

Figure 3 Electrochemical responses of different modified electrodes in 2 mL PBS solution: (a) bare GCE (b) g-C_3N_4@Au@Fc-NH_2/GCE (c) A2+A3/g-C_3N_4@Au@Fc-NH_2/GCE (d) HT/A2+A3 /g-C_3N_4@Au@Fc-NH_2/GCE (e) DNA hydrogel/HT/A2+A3/g-C_3N_4@Au@Fc-NH_2/GCE.

Comparison of Current Response Under Different Conditions In order to prove that only the S1-target-S2 construction was able to achieve homogeneous entropy catalytic amplification, the S1-target, S2-target, S1 and S2 were performed as the contrast respectively for the detection of target protein at the same condition and the results were displayed in the Figure 4. When the electrode was modified with HT/A2+A3/g-C_3N_4@Au@Fc-NH_2, the current peak was presented with curve a. Nevertheless, there were no obvious decrease in the current peaks when S1-target (curve b), S2-target (curve c), S1 and S2 (curve d) appeared in this system compared with the presence of S1-target-S2 (curve e). Thus, we can conclude that S1-target, S2-target, S1 and S2 were not able to induce homogeneous entropy catalytic

amplification, only the formation of S1-target-S2 could realize the purpose of target detection. Moreover, these results also informed that excess S1 or S2 had no effects on this detection system.

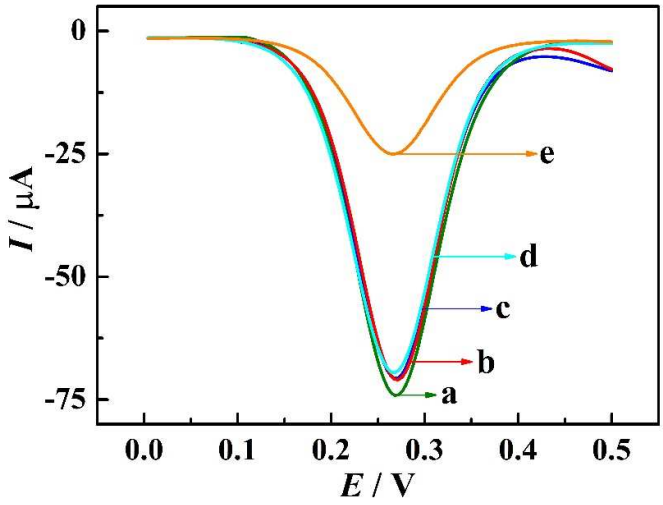

Figure 4 The electrochemical signal intensity for the introduction of S1-target-S2 (e), S1-target (b), S2-target (c), S1 and S2 (d) to form DNA hydrogel incubated onto the modified electrode HT/A2+A3/g-C_3N_4@Au@Fc-NH_2/GCE (a).

Analytical Performance of the Proposed Biosensor for PDGF Detection For the purpose of investigating the sensitivity and the potential quantitative application of the designed biosensor, different concentrations of PDGF were monitored by the proposed biosensor under the optimal conditions. As shown in Figure 5A, the electrochemical signal decreased with the PDGF concentration increasing, and presented a strong correlation between the electrochemical response and the logarithm (lg) of PDGF concentration ranged from 0.01 pM to 10 nM with a regression equation expressed as I = -34.147 + 8.383lgc_{PDGF} (Figure 5B). The correlation coefficient was 0.998 and the limit of detection (LOD) was 3.5 fM for PDGF detection (LOD = 3S_b/m, where m is the slope of the corresponding calibration curve and S_b is the standard

deviation of the blank signals). The analytical performance of this designed biosensor was compared with other previous methods for PDGF detection (Table 1). As a result, the designed biosensor exhibited good analytical performance, attributing to well film-forming electroactive nanomaterials g-C_3N_4@Au@Fc-NH_2 and homogeneous entropy catalytic-driven DNA hydrogel.

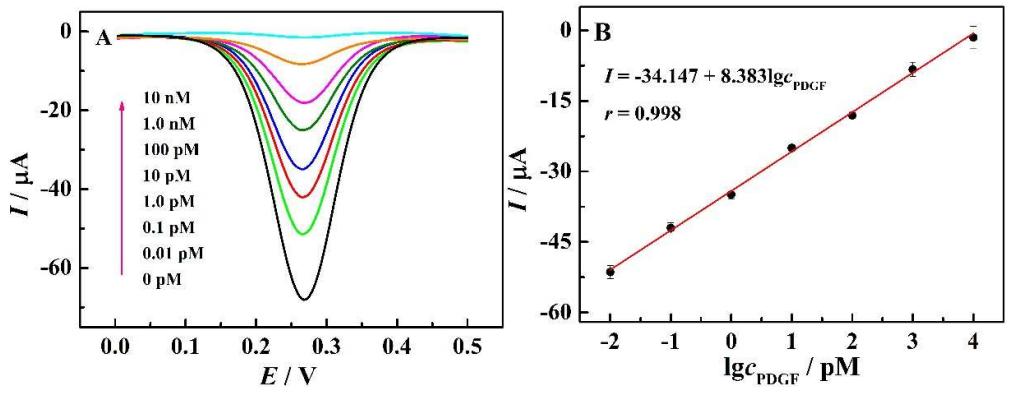

Figure 5 (A) Electrochemical responses of this proposed biosensor incubated with different concentrations of target including 0.01 pM, 0.1 pM, 1.0 pM, 10 pM, 100 pM, 1.0 nM, 10 nM and (B) Calibration curve corresponding to the electrochemical intensity as a function of the logarithm concentration of PDGF in 2 mL PBS (pH=7.0).

Table 1 Comparison of the proposed assay with other methods for PDGF detection.

Analytical method	Linear ranger	The limit of detection	References
Single-channel current	500 fM ~ 10 nM	500 fM	34
Fluorescence	1.0 pM ~ 1000 nM	0.3 pM	35
Colorimetric	2.0 nM ~ 80 nM	1.1 pM	36
Photoinduced electron transfer	0.5 pM~10 nM	0.1 pM	37
Differential pulse voltammogram	17 pM~1660 nM	8.3 pM	38
Chemiluminescence	1.0 pM ~ 1000 pM	0.92 pM	39
Electrochemiluminescent	0.02 ~ 80 nM	0.013 nM	40
SWV	10 fM~10 nM	3.5 fM	this work

Reproducibility, Selectivity and Stability of the Proposed Biosensor In order to investigate the reproducibility, batch-to-batch precision of the proposed biosensor

toward different concentrations (low, middle, high) of PDGF including 0.5 pM, 10 pM and 500 pM was studied, and the relative strandard deviations (RSD) were 5.7%, 4.6% and 6.1% (n = 3) respectively, demonstrating the acceptable accuracy and reproducibility of this proposed assay. For further exploring the selectivity of this proposed biosensor, human immunoglobulins G (IgG), TB (thrombin), and carcinoembryonic antigen (CEA) were adopted as interfering agents. As shown in Figure 6, no significant electrochemical responses of IgG (1.0 nM), TB (1.0 nM) and CEA (1.0 nM) were observed except that for target PDGF (10 pM), while the current signal of the mixture containing IgG (1.0 nM), TB (1.0 nM), CEA (1.0 nM) and PDGF (10 pM) was similar with that of PDGF (10 pM), which implying the good selectivity of this method for PDGF detection. Moreover, the stability of this biosensor was monitored by the prepared fresh electrodes, and the electrochemical signals were measured after 5d (98.13%), 10d (96.92%), 15d (94.25%), 20d (93.89%) and 25d (92.78%). These results proved the proposed biosensor owed good stability.

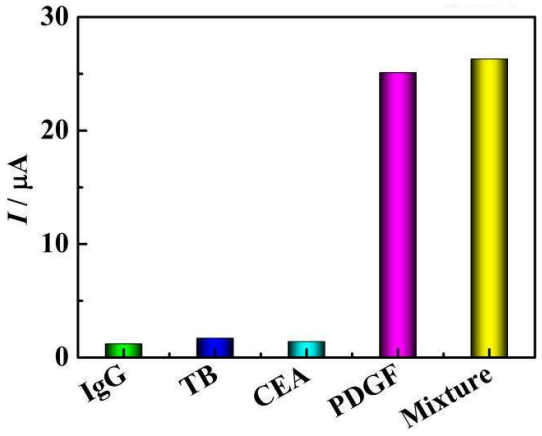

Figure 6 Specificity of this proposed electrochemical biosensor for the introduction of IgG (1.0 nM), TB (1.0 nM), CEA (1.0 nM) and PDGF (10 pM) and the mixture containing IgG (1.0 nM), TB (1.0 nM), CEA (1.0 nM) and PDGF (10 pM).

CONCLUSION

In summary, the present work has demonstrated a novel biosensor depended on homogeneous entropy catalytic-fueled DNA hydrogel as strong signal blocker to significantly hinder the electrochemical signal of electroactive nanomaterials g-C_3N_4@Au@Fc-NH_2 with good-filming for sensitive detection of PDGF. The developed electrochemical biosensor shows three attractive features. First, nanomaterials g-C_3N_4@Au@Fc-NH_2 with good-filming directly were immobilized onto the electrode surface as signal tag, shortening the distance from electrode and providing the strong original signal, and improving the detection accuracy and sensitivity. Secondly, the reliable homogeneous entropy catalytic recycling amplification could convert target protein input into large numbers of nucleic acid outputs, which significantly increased the detection sensitive. Thirdly, the released recycling products of DNA sequences were further amplified by the formation of DNA hydrogel, which intensely hindered the electron transfer and further enhanced the sensitivity for protein detection. Above all, the proposed biosensor provides a high-efficient way to sensitively detect PDGF and possesses great potential for the detection of other proteins by using the corresponding affinity pairs.

ASSOCIATED CONTENT

Supporting Information

Chemicals and materials, apparatus, electrochemical characterization of the proposed biosensor with cyclic voltammetry, and analysis of PDGF in real sample, the oligonucleotide sequences applied in the proposed work (Table S-1),

determination of PDGF added in human blood serum with proposed biosensor (Table S-2), the cyclic voltammetry (CV) characterization of different modified electrodes in 2 mL PBS solution (Figure S-1).

ACKNOWLEDGEMENT

This paper was financially supported by the National Natural Science Foundation of China (21775124, 21675129, 21575116 and 51473136) and the Fundamental Research Funds for the Central Universities (XDJK2017A001, XDJK2018AA003), China.

REFERENCES

(1) Samanta, D., Sarkar, A., *Chem. Soc. Rev.*, **2011**, 40, 2567-2592.

(2) Makaraviciute, A., Ramanaviciene, A., *Biosens. Bioelectron.*, **2013**, 50, 460-471.

(3) Xie, Q. F., Weng, X. H., Lu, L. J., Lin, Z. Y., Xu, X. W., Fu, C. L., *Biosens. Bioelectron.*, **2016**, 77, 46-50.

(4) Povedano, E., Cincotto, F. H., Parrado, C., Díez, P., Sánchez, A., Canevari, T. C., Machado, S. A. S., Pingarrón, J. M., Villalonga, R., *Biosens. Bioelectron.*, **2017**, 89, 343-351.

(5) Tang, Z. Y., He, J. L., Chen, J., Niu, Y. Z., Zhao, Y. L., Zhang, Y. C., Yu C., *Biosens. Bioelectron.*, **2018**, 101, 253-259.

(6) Wu, H., Wei, T., Li, X., Yang, J., Zhang, J., Fan, S. H., Zhang, H., *J Electrochem. Soc.*, **2017**, 164, B147-B151.

(7) Chen, M., Zhao, C. F., Chen, W., Weng, S. H., Liu, A. L., Liu, Q. C., Zheng, Z. F., Lin, J. H., Lin, X. H., *Analyst*, **2013**, 138, 7341-7346.

(8) Huang, K. J., Miao, Y. X., Wang, L., Gan, T., Yu M., Wang, L. L., *Process Biochem.*, **2012**, 47, 1171-1177.

(9) Salazar, P., Martín, M., Roche, R., O'Neill, R. D., González-Mora, J. L., *Electrochim. Acta*, **2010**, 55, 6476-6484.

(10) Salazar, P., Martín, M., Roche, R., González-Mora, J. L., O'Neill, R. D., *Biosens. Bioelectron.*, **2010**, 26, 748-753.

(11) Zuo, X. L., Xiao, Y., Plaxco, K. W., *J. Am. Chem. Soc.*, **2009**, 131, 6944-6945.

(12) Xiong, E. H., Li, Z. Z., Zhang, X. H., Zhou, J. W., Yan, X. X., Liu, Y. Q., Chen, J. H., *Anal. Chem.*, **2017**, 89, 8830-8835.

(13) Rafiee-Pour, H. A., Behpour, M., Keshavarz, M., *Biosens. Bioelectron.*, **2016**, 77, 202-207.

(14) Zhang, S. Y., Garcia-ĎAngeli, A., Brennand, J. P., Huo, Q., *Analyst*, **2014**, 139, 439-445.

(15) Zhang, H. Q., Li, F., Dever, B., Li, Xi. F., Le, X. C., *Chem. Rev.*, **2013**, 113, 2812-2841.

(16) Al-Ogaidi, I., Gou, H. L., Aguilar, Z. P., Guo, S. W., Melconian, A. K., Al-kazaz, A. K. A., Meng, F. K., Wu, N. Q., *Chem. Commun.*, **2014**, 50, 1344-1346.

(17) Abbaspour, A., Norouz-Sarvestani, F., Noori, A., Soltani, N., *Biosens. Bioelectron.*, **2015**, 68, 149-155.

(18) Sung, Y. J., Suk, H. J., Sung, H. Y., Li, T. H., Poo, H., Kim, M. G., *Biosens. Bioelectron.*, **2013**, 43, 432-439.

(19) Liu, X. J., Li, W., Hou, T., Dong, S. S., Yu, G. H., Li, F., *Anal. Chem.*, **2015**, 87, 4030-4036.

(20) Weibrecht, I., Lundin, E., Kiflemariam, S., Mignardi, M., Grundberg, I., Larsson, C., Koos, B., Nilsson, M., Söderberg, O., *Nat. Protoc.*, **2013**, 8, 355-372.

(21) Liu, B. Q., Zhang, B., Chen, G. N., Yang, H. H., Tang, D. P., *Anal. Chem.*, **2014**, 86, 7773-7781.

(22) Kahan-Hanum, M., Douek, Y., Adar, R., Shapiro, E., *Sci. Rep.*, **2013**, 3, 1535.

(23) Liu, W. L., Li, J. P., Wu, Y. X., Xing, S., Lai, Y. Z., Zhang, G., *Biosens. Bioelectron.*, **2018**, 102, 204-210.

(24) Kim, D., Garner, O. B., Ozcan, A., Carlo, D. D., *ACS Nano*, **2016**, 10, 7467-7475.

(25) Liu, S. P., Su, W. Q., Li, Y. L., Zhang, L. L., Ding, X. T., *Biosens. Bioelectron.*, **2018**, 103, 1-5.

(26) Cai,W., Xie, S. B., Zhang, J., Tang, D. Y., Tang, Y., *Biosens. Bioelectron.*, **2017**, 98, 466-472.

(27) Xing, Y. Z., Cheng, E. J., Yang, Y., Chen, P., Zhang, T., Sun, Y. W., Yang, Z. Q., Liu, D. S., *Adv. Mater.*, **2011**, 23, 1117-1121.

(28) Lee, J. B., Peng, S. M., Yang, D. Y., Roh, Y. H., Funabashi, H., Park, N., Rice, E. J., Chen, L. W., Long, R., Wu, M. M., Luo, D., *Nat. Nanotechnol.*, **2012**, 7, 816-820.

(29) Wang, Y. Y., Jiang, L. P., Zhou, S. W., Bi, S., Zhu, J. J., *ACS Appl. Mater. Interfaces*, **2016**, 8, 26532-26540.

(30) Li, J., Mo, L. T., Lu, C. H., Fu, T., Yang, H. H., Tan, W. H., *Chem. Soc. Rev.*, **2016**, 45, 1410-1431.

(31) Bi, S., Yue, S. Z., Zhang, S. S., *Chem. Soc. Rev.*, **2017**, 46, 4281-4298.

(32) Bi, S., Yue, S. Z., Wu, Q., Ye, J. Y., *Chem. Commun.*, **2016**, 52, 5455-5458.

(33) Wang, B. X., Wang, H. J., Zhong, X., Chai, Y. Q., Chen, S. H., Yuan, R., *Chem. Commun.*, **2016**, 52, 5049-5052.

(34) Zhang, L., Zhang, K. X., Liu, G. C., Liu, M. J., Liu, Y., Li, J. H., *Anal. Chem.*, **2015**, 87, 5677-5682.

(35) Wang, X. F., Ishii, Y., Ruslinda, A. R., Hasegawa, M., Kawarada, H., *ACS Appl. Mater. Interfaces*, **2012**, 4, 3526-3534.

(36) Zhang, H. G., Li, F. Y., Chen, H. L., Ma, Y. H., Qi, S. D., Chen, X. G., Zhou, L., *Sens. Actuators B*, **2015**, 207, 748-755.

(37) Wang, G. F., Zhu, Y. H., Chen, L., Zhang, X. J., *Biosens. Bioelectron.*, **2015**, 63, 552-557.

(38) Song, W., Li, H., Liang, H., Qiang, W. B., Xu, D. K., *Anal. Chem.*, **2014**, 86, 2775-2783.

(39) Zou, P., Liu, Y. L., Wang, H. Y., Wu, J., Zhu, F. F., Wu, H., *Biosens. Bioelectron.*, **2016**,79, 29-33.

(40) Xu, H. F., Liang, S. J., Zhu, X., Wu, X. Q., Dong, Y. Q., Wu, H. S., Zhang, W. X., Chi, Y. W., *Biosens. Bioelectron.*, **2017**, 92, 695-701.

For TOC only

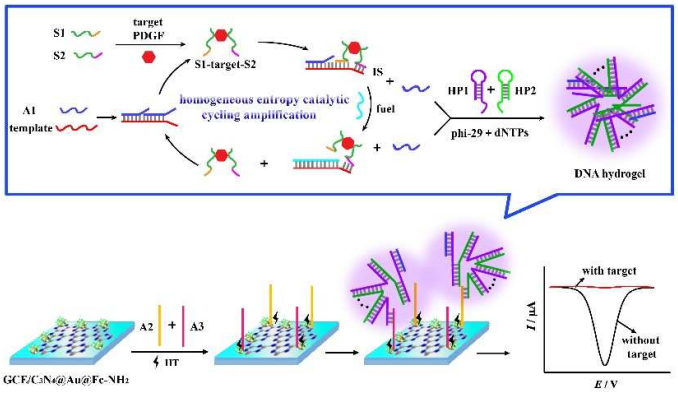
S1
S2
target
PDGF
S1-target-S2
IS
A1
template
homogeneous entropy catalytic
cycling amplification
fuel
HP1
HP2
phi-29 + dNTPs
DNA hydrogel
A2
A3
ITT
GCE/C3N4@Au@Fc-NH2
with target
without
target
I / μA
E / V